Recognition of Some Modulated Apertures Using the Cascaded Fabry- Perot Interferometer(CFPI)

A.M. Hamed
Physics Department, Faculty of Science,
Ain Shams University, 11566 Cairo, Egypt.

ABSTRACT
In this paper, five modulated apertures are considered. The first has linear distribution, the second has conic shape, the third has quadratic distribution, the fourth has Gaussian distribution, and the fifth has B/W concentric annuli. These apertures are recognized from the fringe shift occurred in the interferometric images using the CFPI. The recognized modulated apertures are compared with the fringe shift corresponding to the uniform circular aperture. The improved multiple beam Interferometer or the CFPI working in transmission is considered for the aperture recognition. The sharp interferometric images obtained from the CFPI provided with the apertures are constructed using Mat-Lab code.

Keywords: aperture recognition,modulated apertures, cascaded Fabry Perot interferometer- improvement of interferometric images.

1. INTRODUCTION
Early, digital speckle pattern interferometric system to monitor surface vibrations and out of plane tilt is presented [1], where the resolution of the system used to measure the out of plane displacement is 1/2 per fringe. The application of a general-purpose image-processing computer system to automatic fringe analysis is presented. The applications considered are strain measurement by speckle interferometry, position location in three axes, and fault detection in holographic nondestructive testing [2]. Recently, image processing of apertures using speckle photography and holography was studied by many authors [3- 7]. While interferometric microsopic and other images are investigated in [8, 15]. In a recent publication by the author [16], multiple pass of two beam interference is considered, while in this study we consider CFPI for the formation of sharp fringes. In this paper, aperture recognition using Cascaded Fabry Perot Interferometer (CFPI) is proposed. We can recognize shape of apertures from the fringe shift. The design of modulated apertures like linear, quadratic, B/W concentric annuli, and Gaussian distributions is made using the Mat- Lab code. Results and discussion is given followed by a conclusion.Early, digital speckle pattern interferometric system to monitor surface vibrations and out of plane tilt is presented [1], where the resolution of the system used to measure the out of plane displacement is 1/2 per fringe. The application of a general-purpose image-processing computer system to automatic fringe analysis is presented. The applications considered are strain measurement by speckle interferometry, position location in three axes, and fault detection in holographic nondestructive testing [2]. Recently, image processing of apertures using speckle photography and holography was studied by many authors [3- 7]. While interferometric microsopic and other images are investigated in [8, 15]. In a recent publication by the author [16], multiple pass of two beam interference is considered, while in this study we consider CFPI for the formation of sharp fringes. In this paper, aperture recognition using Cascaded Fabry Perot Interferometer (CFPI) is proposed. We can recognize shape of apertures from the fringe shift. The design of modulated apertures like linear, quadratic, B/W concentric annuli, and Gaussian distributions is made using the Mat- Lab code. Results and discussion is given followed by a conclusion.

2. THEORETICAL ANALYSIS
A higher order multiple beam interference composed of four cascaded interferometers is schematically represented as in the figure (1). A He- Ne laser beam is spatially filtered and rendering parallel using an objective lens L followed by a pinhole P placed in the short focus of the objective lens, and converging lens L1 placed at the focal plane f from the pinhole. The collimated laser beam passes through the four F.P.I. arranged in series followed by the Fourier transform lens L2 of focal length f2, The Fourier and imaging planes are located as shown in the figure (1).
The intensity distribution in case of ordinary FPI is given by this formula [11]:

$$I(\delta;R) = \frac{T^4}{1+R^4-2R^2\cos(\delta)} \qquad (1)$$

Where T is the transmission coefficient while R is the reflection coefficient of the interferometer. δ , is the phase difference between any two adjacent emerging rays.
While in case of cascaded interferometers, the intensity distribution is the ordinary distribution to the power of N, where N is the number of cascaded interferometers. Then, the intensity distribution in Cascaded Fabry- Perot Interferometer (CFPI) is represented as follows:

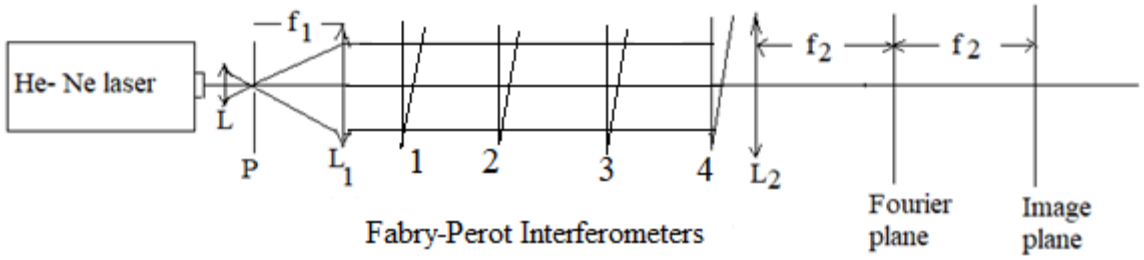

Figure (1): Multiple beam interferometer composed of four cascaded interferometers. L objective lens, P pinhole, and L1 converging lens where the elements L, P, and L1 render the laser beam spatially filtered and collimated. L2 is the Fourier transform lens of focal length f2, The Fourier and imaging planes are shown in the figure.

$$I(\delta; R, N) = [\frac{T^4}{1+R^4-2R^2\cos(\delta)}] \quad (2)$$

The maximum intensity is computed as:

$$I(\delta = 2\pi; R, N) = I_{max}(R, N) = [\frac{T^4}{(1-R^2)^2}]^N \quad (3)$$

Making use of equations (2, 3), the normalized intensity due to the cascaded multiple beam interference can be written as follows:

$$I_{normalized}(\delta; R, N) = \frac{I}{I_{max}} = \frac{1}{[1 + F\,sin^2(\frac{\delta}{2})]^N} \quad (4)$$

Where $F = \frac{4R^2}{(1-R^2)^2}$ is the coefficient of finesse. (5)

F defined as the coefficient of finesse is a measure of fringe sharpness and contrast.

For greater values of reflectivity, R > 80%, F is much larger than one, hence, approximate expression for the intensity is obtained as:

$$I_{normalized}(\delta; R, N) \sim 1/[F\,sin^2\left(\frac{\delta}{2}\right)]^N \quad (6)$$

The five modulated apertures used in the CFPI described above are represented as follows:

$$P(\rho) = \rho \quad ; |\frac{\rho}{\rho_0}| \leq 1 \quad ; \quad \text{for linear aperture} \quad (7)$$

$$P(\rho) = 1 - \rho \quad ; |\frac{\rho}{\rho_0}| \leq \quad ; \quad \text{for conic aperture} \quad (8)$$

$$P(\rho) = \rho^2 \quad ; |\frac{\rho}{\rho_0}| \leq 1 \quad ; \quad \text{for quadratic aperture} \quad (9)$$

$$P(\rho) = \exp\left[-\left(\frac{\rho}{\rho_0}\right)^2\right] \quad ; |\frac{\rho}{\rho_0}| \leq 1 \quad ; \quad \text{for Gaussian aperture} \quad (10)$$

$$P(\rho) = \sum_{i=1}^{N} [\,P_{2i}(\rho) - P_i(\rho)\,] \quad ; |\frac{\rho}{\rho_0}| \leq 1 \quad \text{for black and white concentric annuli} \quad (11)$$

Assume that the apertures described in equations (6- 11) are considered as images represented in matrix form and introduced inside the CFPI, where P ( ) =φ(x, y) = φ(m Δx, n Δy). The image matrix has dimensions of M × N. Where m = 1: 512 and n= 1: 512 pixels. Then, the fringe shift present in the image is located in the harmonic term in the Airy distribution. Hence, equation (2), is rewritten as follows:

$$I(\delta; R, N) = [\frac{T^4}{1+R^4-2R^2\cos[\delta+\varphi(x,y)]}]^N \quad (12)$$

Or using equation (4), we write normalized intensity considering the deformed phase as follows:

$$I_{normalized}(\delta; R, N) = \frac{I}{I_{max}} = \frac{1}{[1 + F\,sin^2(\frac{\delta+\varphi(x,y)}{2})]^N} \quad (13)$$

Now we compute the phase mapping of the image from equation (12) as follows:

The deformed or shifted phase is the sum of the inter-fringe spacing and the image phase represented as follows:

$$\varphi(x,y)_{deformed} = \delta + \varphi(x,y) \quad (14)$$

Consequently, the phase of the image iseasily deduced from equation (13) as follows:

$$\varphi(x,y) = \varphi(x,y)_{deformed} - \pi \quad (15)$$

Where the inter-fringe spacing is given by:

$$\delta = \frac{2\pi}{\lambda}(O.P.D.) = \frac{2\pi}{\lambda}\left(\frac{\lambda}{2}\right) = \pi. \quad (16)$$

Compared with the known method of fringe shift obtained at 0, π/2, π, 3π/2 for successive intensities I1 , I2 , I3, and I4 ,giving this result:

$$\varphi(x,y) = tan^{-1}\left(\frac{I_2 - I_1}{I_4 - I_3}\right) \quad (17)$$

3. RESULTS AND DISCUSSION

The coefficient of finesse F as a function of reflectivity R for different cascaded interferometers is computed from equation (14) and represented as shown in the figure (2). N=1 stands for the ordinary FPI while N= 2, 3, and 4 stands for the number of cascaded interferometers.

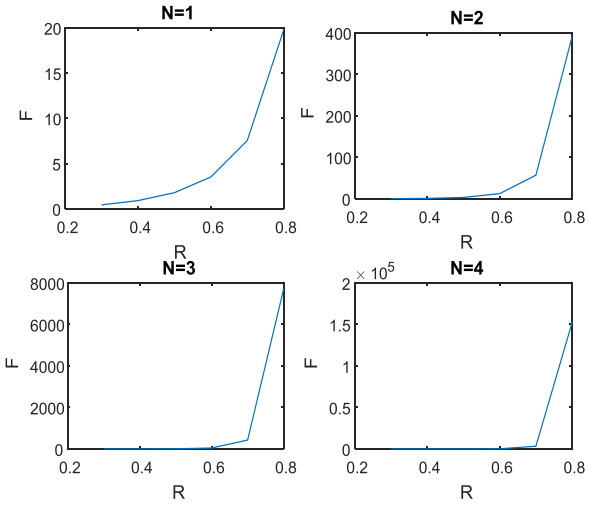

Figure (2): Coefficient of finesse F as a function of reflectivity R for different cascaded interferometers. N=1 stands for the ordinary FPI while N= 2, 3, and 4 stands for the number of cascaded interferometers.

The design of the investigated linear, conic, quadratic, and Gaussian apertures is fabricated using Mat- Lab code. The Linearly distributed aperture of diameter 256 pixels and the matrix dimensions of the whole image 512 × 512 pixels is shown in the figure (3). For the 1st model of linear aperture, it is shown, as in the figure (4- a), that the fringe shift due to the aperture has linear shape which recognizes it. Seven fringes are shown for the whole image while only four shifted fringes appeared inside the aperture. In the figure (4- b), fourteen fringes are shown in the whole image while seven shifted fringes appeared inside the aperture.

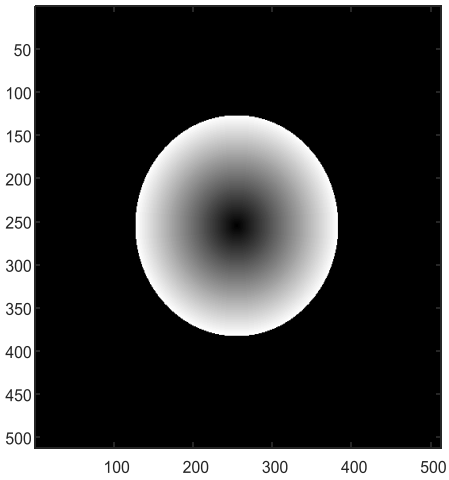

Figure (3): Linearly distributed aperture of diameter 256 pixels and the matrix dimensions of the whole image is 512 × 512 pixels.

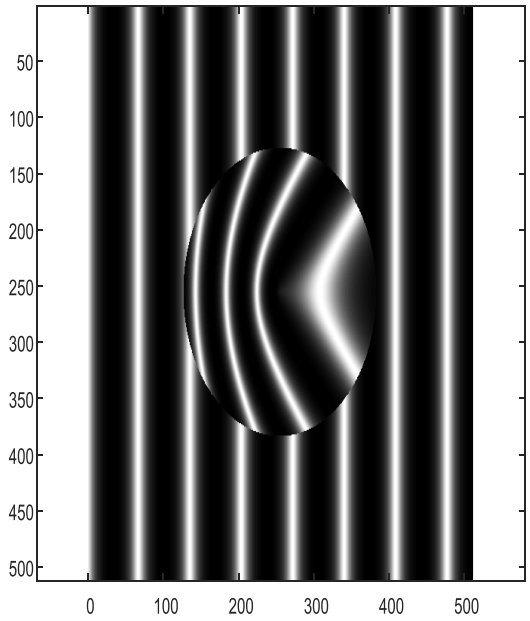

Figure (4- a): The fringe shift has linear shape to identify the linear aperture. Seven fringes are shown for the whole image while only four fringes appeared inside the aperture.

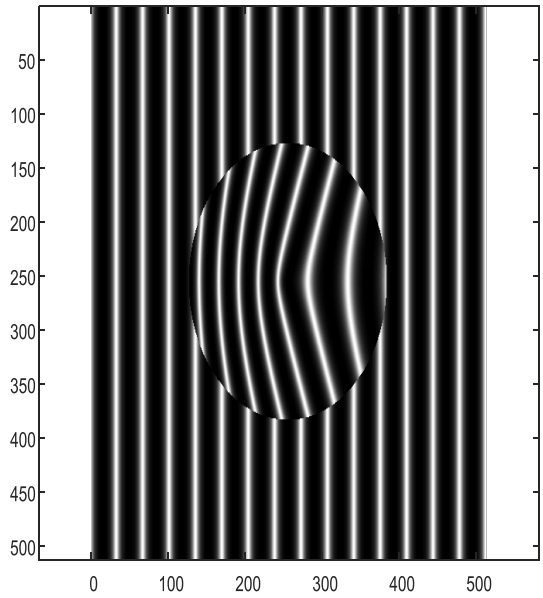

Figure (4- b): Fourteen fringes are shown in the whole image while seven shifted fringes appeared inside the aperture.

In one dimension, the fringe shift corresponding to the linear aperture is shown in the figure (5- a). The fringes give the phase

of the image at different locations where the 2nd fringe, from the right, gives zero shift. Seven fringes are shown in the plot while only four shifted fringes appeared inside the aperture. It is shown, for the linear aperture, that the fringe shift equals the inter-fringe spacing (δZ= ΔZ). In the figure (5- b), the 3rd fringe has zero shift compared with the other straight line fringes giving the phase of the image at different locations. Fourteen fringes are shown in the plot while only eight shifted fringes appeared inside the aperture. For the 2nd model, namely conic aperture where P (□ □) = 1 □ , it is shown that the fringe shift has conic shape as shown in the figure (6). The shift appears in the reverse direction corresponding to the linear aperture. The aperture has diameter =256 pixels and the matrix dimensions of the whole image is 512 × 512 pixels. Seven fringes are shown for the whole image while only four shifted fringes to the right are appeared. The fringe shift in one dimension has conic shape is shown in the figure (7).The shift appears in the reverse direction corresponding to the linear aperture. The aperture has diameter =256 pixels and the matrix dimensions of the whole image is 512 × 512 pixels. Four shifted fringes are shown inside the conic aperture. The mat- Lab code for the conic aperture is written as follows: The Mat- Lab code for the mono-dimensional conic aperture is written as follows:

A (r, c) = 1- ((r- xcen) ^ 2) ^0.5

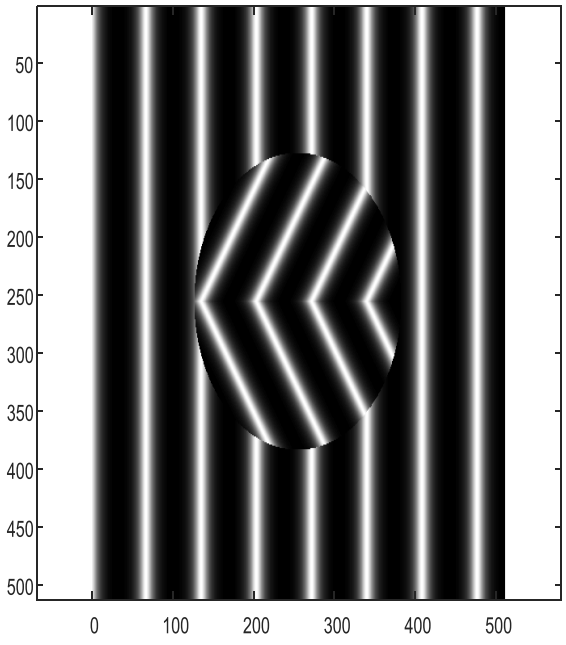

Figure (5-a): The fringe shift corresponding to the linear aperture in one dimension. The fringes give the phase of the image at different locations while the 2nd fringe give zero shift. Seven fringes are shown in the plot while only four fringes appeared inside the aperture. It is shown, for the linear aperture, that the fringe shift equals the inter-fringe spacing (δZ= ΔZ).

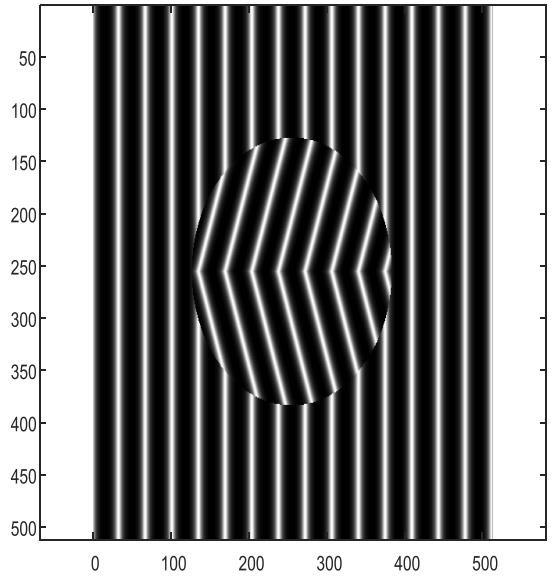

Figure (5- b): The fringe shift in one dimension is shown in the graph. The 3rd fringe has zero shift compared with the other straight line fringes giving the phase of the image at different locations. Fourteen fringes are shown in the plot while only eight fringes appeared inside the aperture.

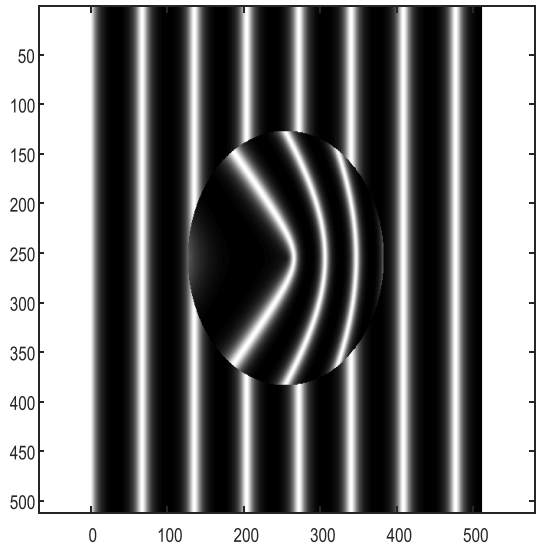

Figure (6): The fringe shift has conic shape. The shift appears in the reverse direction corresponding to the linear aperture. The aperture has diameter =256 pixels and the matrix dimensions of the whole image is 512 × 512 pixels. Seven fringes are shown.

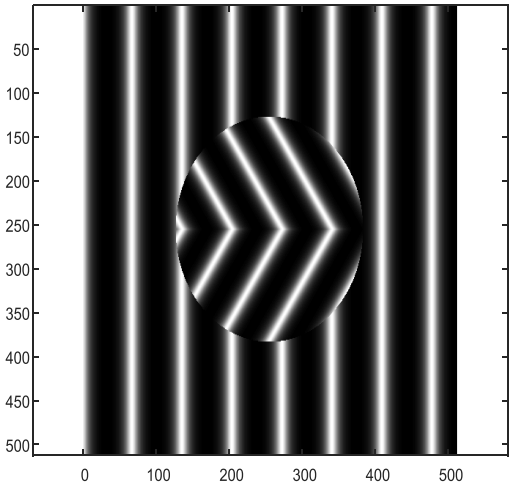

Figure (7): The fringe shift in one dimension has conic shape.The shift appears in the reverse direction corresponding to the linear aperture. The aperture has diameter =256 pixels and the matrix dimensions of the whole image is 512 × 512 pixels. Four fringes are shown inside the conic aperture.

An aperture in the form P (□) = □1.1 is shown as in the figure (8- a). This aperture is deviated from linearity by 10%. The corresponding fringe shift is not linear, hence any deviation from linearity give quadratic fringe shift as shown in the figure (8- b). The Mat- Lab code for the aperture deviated from linear distribution by 10% is:

A(r,c)= (sqrt ((r-xcen)^2 + (c-ycen)^2))^1.1 ;

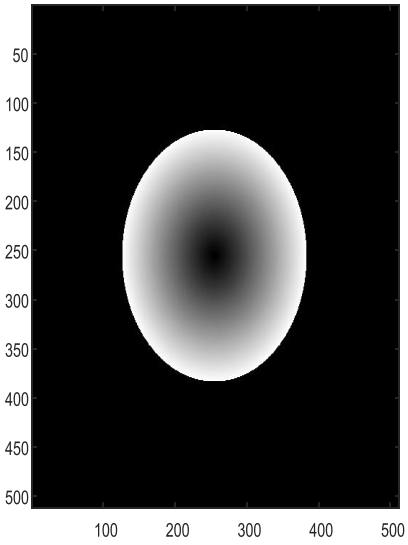

Figure (8- a): An aperture in the form P $(\rho) = \rho^{1.1}$ is shown is shown in the graph

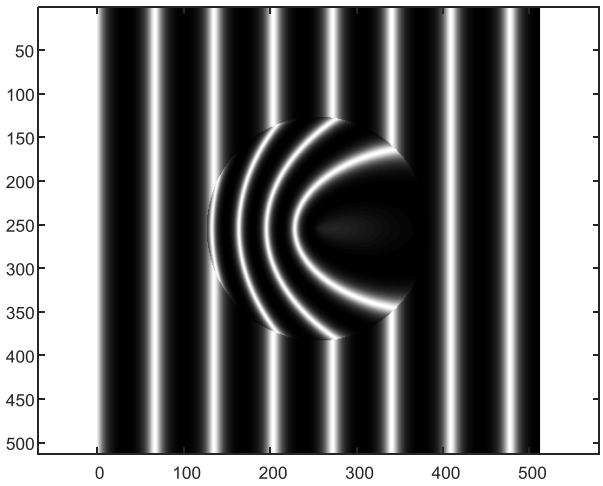

Figure (8- b): The quadratic fringe shift corresponding to an aperture in the form P $(\rho) = \rho^{1.1}$ The Mat- Lab code for the aperture is:
A(r,c)= (sqrt ((r-xcen)^2 + (c-ycen)^2))^1.1 ;

The investigation of the fringe shift for this aperture in one dimension is outlined as in the figure (9 a- c).The fringe shift in case of one direction for nearly linear aperture is shown as in the figure (9- a) where the cursor stands at the point x1 = 272 pixels for the 4th fringe from the right. In the figure (9- b), the cursor stands at the point x1 = 204 pixels for the 5th fringe from the right. Hence, the inter-fringe spacing is deduced as: ΔZ= 272- 204 = 68 pixels. Figure (9- c) represents the fringe shift in case of one direction for nearly linear aperture and the cursor stands at the point x1 = 197 pixels for the shifted fringe. The amount of fringe shift for this deviated aperture from linearity is: δZd = 275- 197 = 68 pixels. The differential fringe shift is:
(δZd - ΔZ)/ΔZ =(75-68)/68 = 0.102.

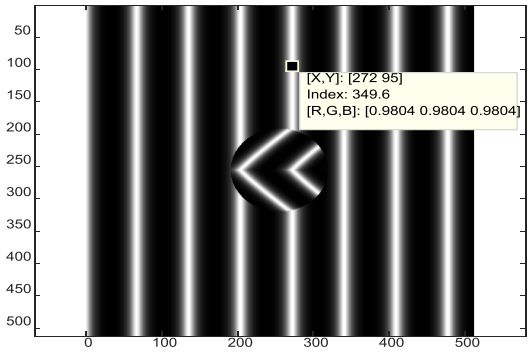

Figure (9- a): The fringe shift in case one direction for nearly linear aperture and the cursor stands at the point x1 = 272 pixels for the 4th fringe from the right.

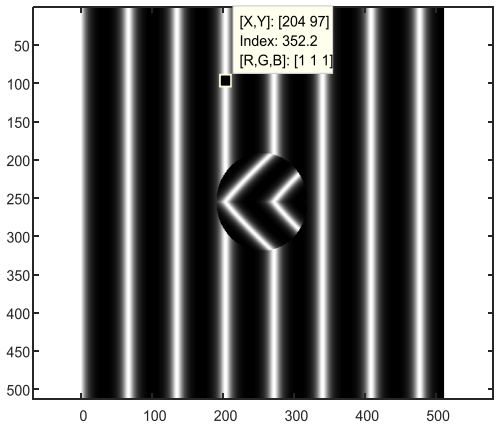

Figure (9- b): The fringe shift in case one direction for nearly linear aperture and the cursor stands at the point x1 = 204 pixels for the 5th fringe from the right. The inter-fringe spacing is deduced from figure (7 a, b) as: ΔZ= 272-204 = 68 pixels.

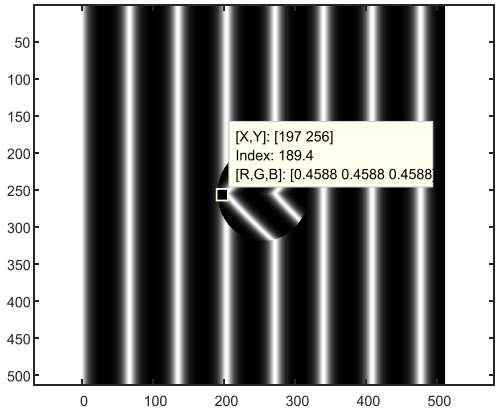

Figure (9- c): The fringe shift in case of one direction for nearly linear aperture and the cursor stands at the point x1 = 197 pixels for the shifted fringe. The amount of fringe shift for this deviated aperture from linearity is: δZd = 275- 197 = 68 pixels. The differential fringe shift is: (δZ - ΔZ)/ΔZ =(75-68)/68 = 0.102. This differential fringe shift is related to the deviated aperture from linearity.

For the 3rd model, Quadratic aperture of diameter 256 pixels. is shown as in the figure (10- a). Interference fringes modulated by mono-dimensional quadratic aperture of diameter 256 pixels is shown as in the figure (10- b). Mat- Lab code of the aperture is represented as follows: A(i, j)= ((i- xcen)^2)/256 ;where i= 1:512, j= 1: 512 pixels, andxcen = 256 pixels. Another interference fringes modulated by mono-dimensional quadratic aperture of diameter 256 pixels of different amplification is shown as in the figure (10- c). The corresponding Mat- Lab code of the aperture is:

A(i, j)= ((i- xcen)^2)/1024 ;where i, j, and xcen are as in figure (10- b).

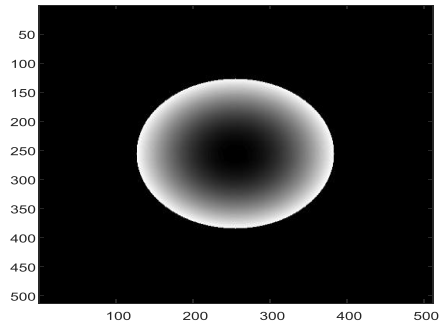

Figure (10- a): Quadratic aperture of diameter 256 pixels.

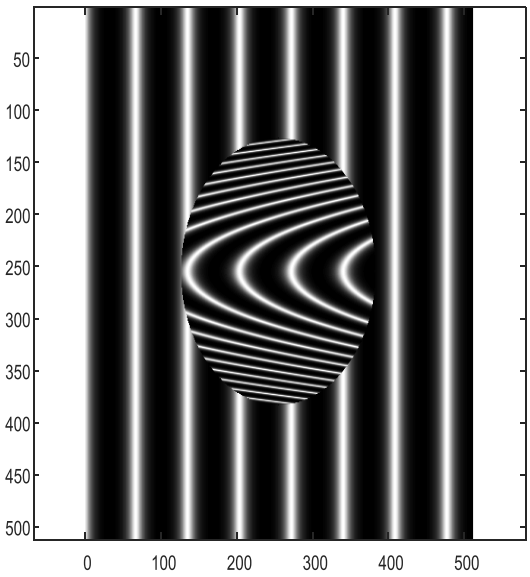

Figure (10- b): Interference fringes modulated by mono-dimensional quadratic aperture of diameter 256 pixels. The Mat- Lab code of the aperture is: A(i, j)= ((i- xcen)^2)/256 ;where i= 1:512, j= 1: 512 pixels. xcen = 256 pixels.

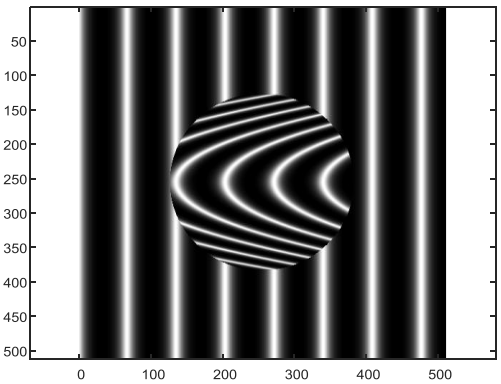

Figure (10- c): Interference fringes modulated by mono-dimensional quadratic aperture of diameter 256 pixels.

The Mat- Lab code of the aperture is: A(i, j)= ((i- xcen)^2)/1024 ;where i= 1:512, j= 1: 512 pixels. xcen = 256 pixels.

The 4th model of Gaussian aperture of truncation radius R= 64 pixels. is shown as in the figure (11- a). The Mat- Lab code for the Gaussian aperture is written as follows:

A(i, j)= G* exp (-((i- xcen)^2 + (j- ycen)^2)/R^2); G = 4

The fringe shift corresponding to the Gaussian aperture inside a circle of diameter 256 pixels is shown as in the figure (11- b). Where the aperture has radius R= 64 pixels and G= 4. The fringe shift for the Gaussian aperture for G = 8, is shown in the figure (11- c).Another plot of the fringe shift inside a circle of diameter 512 pixels for the Gaussian aperture of radius R= 128 pixels is shown as in the figure (11- d). It is shown from all the plots shown in the figure (11 b- c) that the distribution is Gaussian.

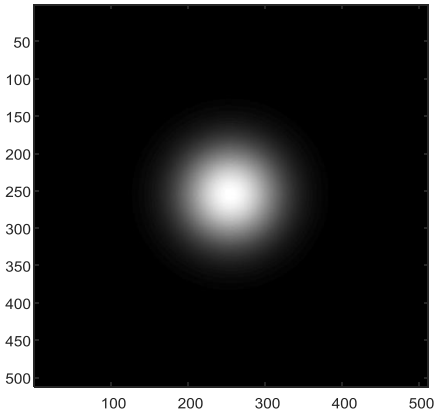

Figure (11- a): Gaussian aperture of truncation radius R= 64 pixels.

The Mat- Lab code for the Gaussian aperture
A(i, j)= (4)* exp (-((i- xcen)^2 + (j- ycen)^2)/R^2);

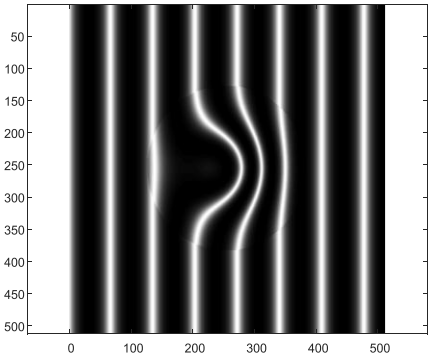

Figure (11- b): The fringe shift corresponding to the Gaussian aperture inside a circle of diameter 256 pixels. The aperture radius R= 64 pixels.
A(i,j)= G* exp (-((i- xcen)^2 + (j- ycen)^2)/R^2); G = 4

The Mat- Lab code for the fringe shift corresponding to the Gaussian aperture is: F1 = 4*r1^2*(sin (0.5*y – A (i, j))^2);

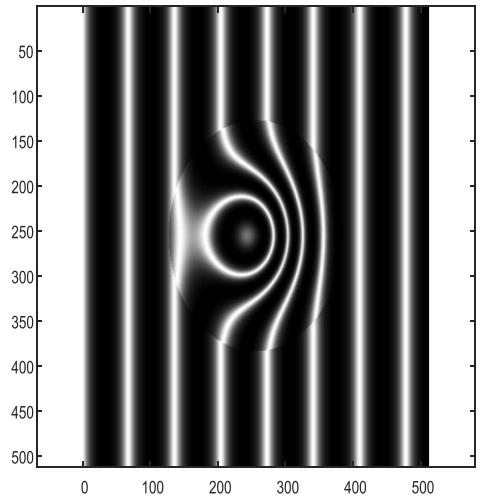

Figure (11- c): A(i,j)= G* exp (-((i- xcen)^2 + (j- ycen)^2)/R^2); G = 8

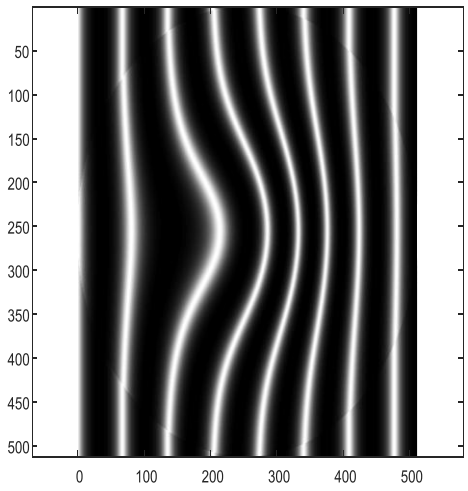

Figure (11- d): The fringe shift inside a circle of diameter 512 pixels for the Gaussian aperture of radius R= 128 pixels.

The B/W concentric annuli are shown as in the figure (12- a). It has four equal transparent annuli in succession with four equal black annuli. The fringe shift corresponding to B/W concentric annuli has shifted discontinuous straight line fringes as shown in the figure (12- b).

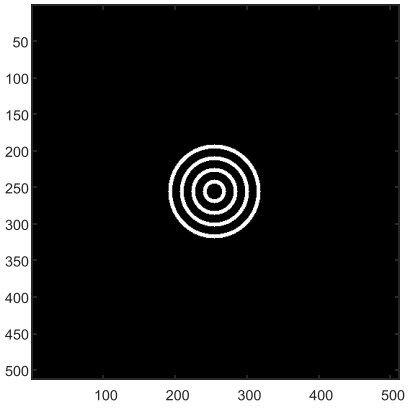

Figure (12- a): The aperture of B/W concentric annuli. It has four equal transparent annuli in succession with four equal black annuli.

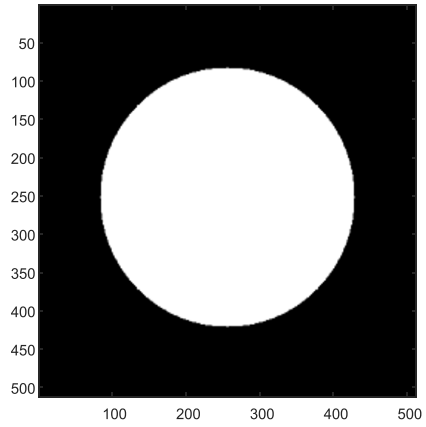

Figure (13- a): Uniform circular aperture of constant transmittance. The aperture has diameter of 256 pixels.

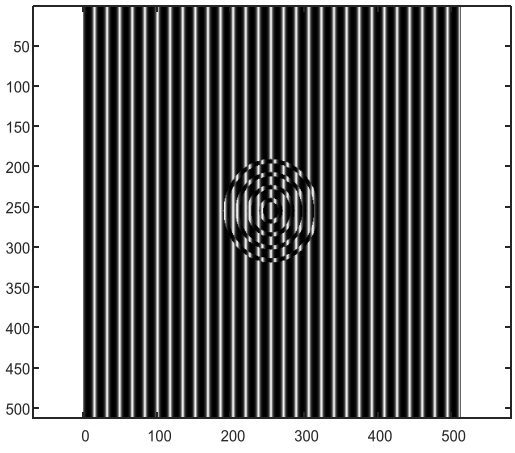

Figure (12- b): The fringe shift corresponding to B/W concentric annuli. It has shifted straight line fringes.

The comparison of the fringe shift for the modulated apertures with the uniform circular aperture is shown as in the figures (13 a, b).Uniform circular aperture of constant transmittance of diameter of 256 pixels is shown in the figure (13- a), while a shifted straight line fringes of constant value identifies the uniform circular aperture as shown in the figure (13- b).

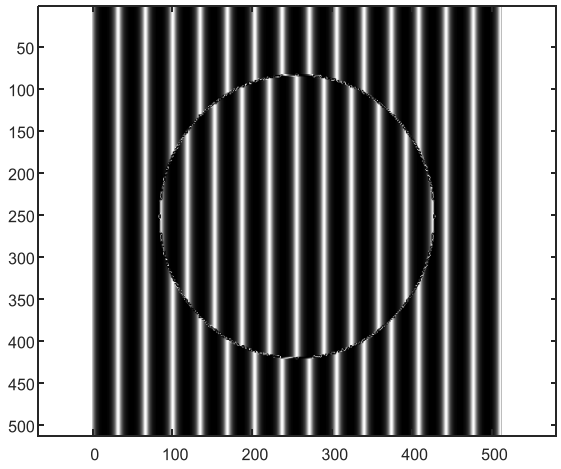

Figure (13- b): Shifted straight line fringes of constant value identifies the uniform circular aperture shown in the figure (a).

4. CONCLUSION

We conclude that the selected models of apertures are recognized referring to the corresponding fringe shift. It is shown linear fringe shift corresponding to the linearly distributed aperture.The aperture with conic distribution has similar linear fringe shift corresponding to the linearly distributed aperture butin opposite direction. While quadratic fringe shift manifests recognition of quadratically distributed aperture. Finally, the Gaussian fringe shift recognizes the Gaussian aperture which is characteristic of the laser beam propagation. The B/W concentric annuli has constant discontinuous fringe shift. The comparison with uniform circualr aperture which gives constant shift is given. The deviation from the linearly distributed aperture by an amount 10% transforms the fringe shift from linear to quadratic variation.

REFERENCE

[1] Chandra Shakher, K. Matsuda, et. al. Proceedings of ICICS, 12 Sept. 1997.
[2] David W. Robinson, Appl. Opt. 22(1983) 2169- 2176, Automatic fringe analysis with a computer image processing system.
[3] A. M. Hamed, Journal of Modern Optics, 56, (2009) 1174-1181, Numerical Speckle Images Formed by Diffusers Using Modulated Conical and Linear Apertures. http://dx.doi.org/10.1080/09500340902985379
[4] A. M. Hamed, Journal of Modern Optics, 56(2009)1633-1642, Formation of Speckle Images Formed for Diffusers Illuminated by Modulated Apertures (Circular Obstruction). http://dx.doi.org/10.1080/09500340903277792
[5] A. M. Hamed, Optical Engineering, 50(2011) 1- 7, Discrimination between Speckle Images Using Diffusers Modulated by Some Deformed Apertures: Simulation. http://dx.doi.org/10.1117/1.3530085
[6] A. M. Hamed, Optics and Photonics Journal ,1(2011) 43-51, Computer Generated Quadratic and Higher Order Apertures and Its Application on Numerical Speckle Images. http://dx.doi.org/10.4236/opj.2011.12007
[7] A. M. Hamed, Precision Instrument and Mechanology (PIM), 3 (2014) 144- 152, Study of Graded Index and Truncated Apertures Using Speckle Images.
[8] A. M. Hamed, Optics and Photonics Journal, 6(2016),Image Processing of Corona Virus Using Interferometry.DOI: 10.4236/opj.2016.65011
[9] J. C. Wyant, Applied Optics ,52 (2013) 1- 8, Computerized Interferometric Surface Measurements. http://dx.doi.org/10.1364/AO.52.000001
[10] J. H. Bruning,D. R. Herriott, J. E. Gallagher, et al.,Applied Optics, 13, (1974) 2693-2703, Digital Wave-Front Measuring Interferometer for Testing Optical Surfaces and Lenses.http://dx.doi.org/10.1364/AO.13.002693
[11] T. Yatagai,,and S. Nakadate, Optical Engineering, 21 (1982) 432-435, Automatic Fringe Analysis Using Digital Image Processing Technique.
[12] A. M. Hamed, www.lap.com (Lambert Academic Publishing), 14 Nov. (2017), The Point Spread Function of some modulated apertures (Application on speckle and interferometry images) ISBN:9786202070706.
[13] A.M. Hamed, Int. J. Innovative Res. in Computer Science and Tech (IJIRCST), 4 (2016)38- 45, Investigation of SIDA Virus (HIV) images using interferometry and speckle techniques.
[14] A.M. Hamed, Opt. and Photonics J. 6 (2016)75- 86, Image processing of coronavirus using interferometry.
[15] A.M. Hamed, Topics on optical and digital image processing using holography and speckle techniques, publisher by Lulu.com, ISBN 9781329328464 Nov. 29, 2015.
[16] A.M. Hamed, Int. J. Photonics and Optical Technology (IJPOT) 3(2017), A Modified Michelson Interferometer and an Application on Microscopic Imaging.

